WAVELET DESCRIPTORS FOR OBJECT RECOGNITION USING MEXICAN HAT FUNCTION

Adnan Abou Nabout[*] **Bernd Tibken**[**]

[*, **] *Chair of Automatic Control, Faculty of Electrical, Information and Media Engineering,*
University of Wuppertal Rainer-Gruenter-Str. 21, 42119 Wuppertal, Germany,
e-mail: {nabout,tibken}@uni-wuppertal.de

Abstract: In this paper, we propose an object recognition method for 2D objects using wavelet descriptors. The descriptors are derived from the continuous wavelet transform using the Mexican hat function as mother wavelet. In contrast to the other known methods we apply an angle function to describe object contours extracted as polygons. The contour extraction is based on the object oriented contour extraction method (OCE). The polygon representation is based on the curvature dependent contour approximation (CDCA). The continuous wavelet transform (CWT) is used in order to apply a suitable number of wavelet descriptors (WD), which are qualified to characterize the object shapes. *Copyright © 2005 IFAC*

Keywords: Image Processing, Object Recognition, Feature Extraction, Fourier Transformation, Wavelet Transformation.

1. INTRODUCTION

The automatic recognition of objects is a widespread application in image processing and pattern recognition systems. One of the most important tasks in this application is the representation of object shapes by a number of specific features.

Many methods have been proposed to describe object shapes. Several methods use segment sequences composed with different segment types like chain code (Freeman, 1974) or segments of constant curvature (Ramer, 1972). Rodenacker, *et al.* (1987) used the so-called shape factor. A shape factor includes measurements of the object like moments, area, perimeter etc. Advanced methods use descriptors derived from Fourier transformation (Granlund, 1972; Zahn and Roskies, 1972) or wavelet transform (Chunag and Kuo, 1996; Feng and Bui 2001).

Fourier descriptors (FD) have been a powerful tool for pattern recognition. Such FD are derived using Fourier transform (FT) of one or two dimensional functions, which describe the object shape. The recognition is then based on the comparison between the FD of the unknown object with those of the stored prototypes using minimum distance (Nabout 1992) or Fuzzy methods (Nabout, *et al.*, 1994).

To checkout the CWT about its ability of describing object shapes, similar to FT, we show in this paper the derivation of wavelet descriptors using the Mexican hat function as mother wavelet and the angle function derived from the extracted contour polygon of a given object. The usage of the Mexican hat function allows, similar to the Fourier transformation described in (Granlund, 1972), the execution of the continues wavelet transform in order to apply suitable number of coefficients. Other basis functions like Daubechies, Coiflet; Haar etc. can be used, but they require the execution of the discrete wavelet transform which needs suitable discretization of the object contours and includes consequently some errors.

The paper is organized as follows:
Section 2 shows the method of describing object shapes using an angle function. In this section, the object oriented contour extraction method (OCE) (Nabout, *et al.*, 1993) as well as the description of contours as polygons (Nabout, *et al.*, 1995) are shown. Section 3 indicates the derivation of the wavelet descriptors (WD) using the Mexican Hat function as mother wavelet. Section 4 shows some results of the CWT for different object shapes.

2. SHAPE DESCRIPTION USING the ANGLE FUNCTION

To apply an angle function we at first use the OCE method in order to extract the object contours from the original image and to describe them as chain code. The following processing steps must be done in order to extract the object contours according to the OCE method (Nabout, *et al.*, 1993).

Step 1: Divide the image into 2*2 resp. 4*4 overlapped windows as shown bellow

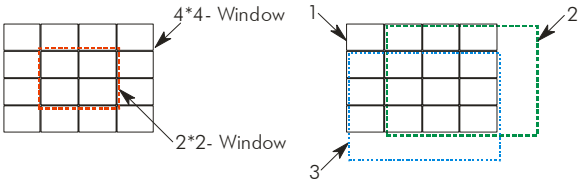

Step 2: Find out the contour edges a_i and their coordinates (x_i, y_i) according to Freeman code (Freeman, 1972) by calculating the pixel values of the windows as given in the following extraction rules.

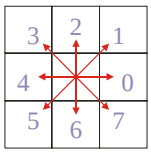

Extraction rules

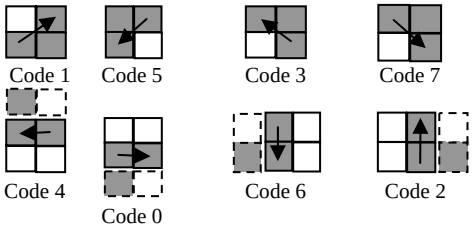

Step 3: Connect the extracted edges to build the contour chains by checking the start and end points of the edges. Fig. 1 shows an example of the connection process.

a_i	x_i	y_i
0	2	2
1	3	2
7	4	1
2	2	3
7	5	2
1	1	4
7	6	3
2	1	5
6	7	4
3	2	6
5	7	5
3	3	7
5	5	6
4	6	6
1	2	8
7	5	6
4	3	8
4	4	8
4	5	8

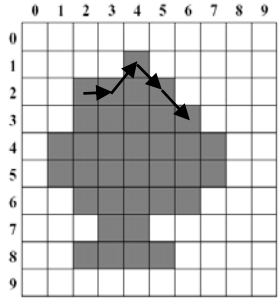

Fig.1 Example of the edge connection

Using the curvature dependent contour approximation (Nabout, *et al.*, 1995), we can describe the contours in the next stage as polygons. This method is working with a splitting and merge algorithm and is qualified to approximate the contours depending on the local curvature. This is necessary to avoid distortion of the contour characteristic, which can destroy the recognition process. The contour approximation using the CDCA method are given in the following five steps.

Step 1
Split the contour chain into regular sequences with max. 2 different Freeman codes.

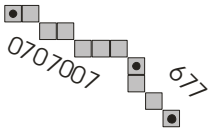

Step 2
Detect noise sequences by calculating the lengths and angle changes of the sequences. The following condition is used to detect noise sequences

$l_{i+1} * \alpha_i \leq 135^\circ$

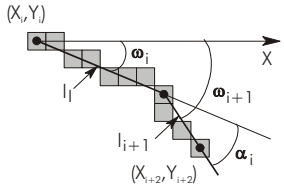

Step3
Build new sequences by merging the noise sequences with regulars.

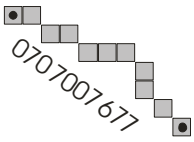

Step4
Split the new sequences iteratively when the following condition
d > dg AND α > αg
(e.g. dg = 1 Pixel and
αg = 1 Degree)
is fulfilled.

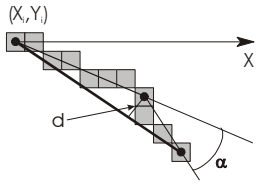

Step5
Connect the start and end points of the sequences resulted from step 4 by lines.

Fig. 2 shows an example of the contour extraction and approximation using OCE (Fig 2a) and CDCA method (Fig 2b) which is described above.

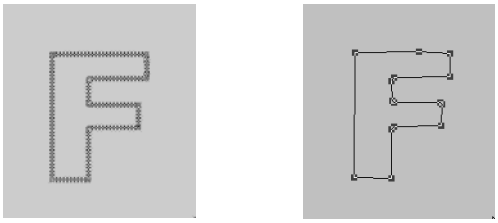

Fig.2 Example results, a) contour extraction, b) contour approximation

As shown in Fig. 2b the number of polygon edges needed to characterize the given object is very low and depends on the curvature of the object. For objects with complex shapes the number of polygon edges will be higher than for the shape of the character F in Fig. 2.

The approximated object in Fig. 2b can be described using an angle function $\phi(l)$ resp. $\phi^*(l)$ defined as following:
Beginning from a starting point on the contour we define the angle function $\phi(l)$ which gives the angle changes along the contour length. The angle changes are represented by the differences between the angle at the current contour position and the angle at the starting point. For the shape of Fig. 2b the angle values changes only at the polygon corners. Therefore $\phi(l)$ is a step function. Fig. 3a shows the step function for the character of Fig. 2.

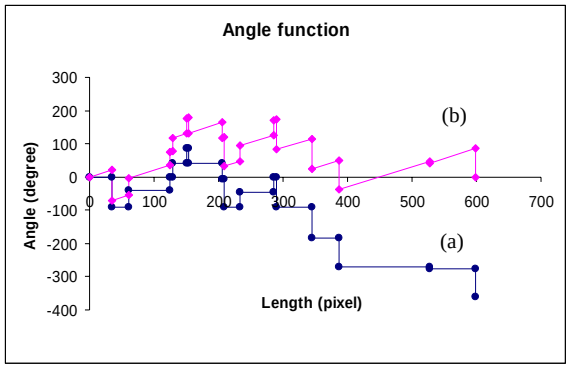

Fig. 3 The angle function $\phi(l)$ (a) and $\phi^*(l)$ (b) of the character of Fig. 2.

Using the following parameter transformation

$$l = Lt/2\pi$$

with

L : Total length of the contour

we can derive a periodical angle function $\phi^*(l)$ as given in the following Equation:

$$\phi^*(t) = \phi(Lt/2\pi) + t \tag{1}$$

This function describes the object shape independent of the size of the object, his position or orientation (Fig 3b).

3. WAVELET TRANSFORMATION

Similar to the FT, the WT uses elementary functions, called wavelets, to describe a given signal (Strang, 1993). In contrast to the FT, which uses harmonic functions with different dilatation, compression and shifting, the WT uses only one basis wavelet (mother wavelet) to derive the reconstruction signals. Likewise through dilatation, compression and shifting of the mother wavelet, we derive new variants of this signal which together build the so called wavelet building set. Equation (2) shows in our case the derived wavelets $\Psi^{a,b}(t)$ from the mother wavelet $\Psi(t)$ (Daubechies, 1992).

$$\Psi^{a,b}(t) = |a|^{-\frac{1}{2}} \Psi\left(\frac{t-b}{a}\right) \tag{2}$$

Where a is the compression or dilatation parameter and b is the shifting parameter. Based on the Mexican Hat function, Fig. 4 shows the mother wavelet and some derived variants resulting from the compression, dilatation and shifting of the mother wavelet using Equation (2) (Strang, 1993).
Similar to the FT, Equation (3) shows the coefficient $W_\Psi \phi^*(a,b)$ of the CWT for the function $\phi^*(t)$

$$W_\Psi \phi^*(a,b) = |a|^{-\frac{1}{2}} \int_{-\infty}^{\infty} \phi^*(t) \Psi\left(\frac{t-b}{a}\right) dt \tag{3}$$

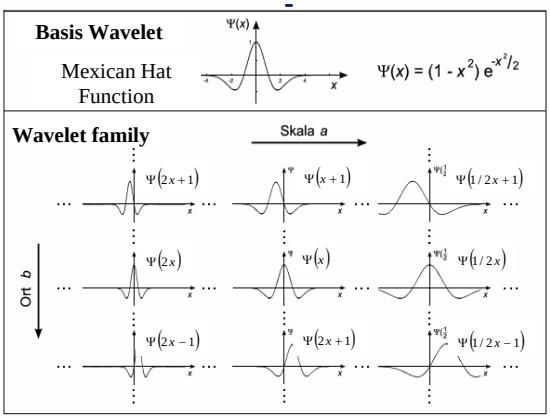

Fig. 4 Wavelet building set based on Mexican Hat

When we substitute the function Ψ in Equation (3) with the Mexican Hat function given below

$$\Psi(t) = (1-t^2)e^{-\frac{t^2}{2}} \tag{4}$$

and limit the integration to the definition interval $[0-2\pi]$, we receive the following expression.

$$W_\Psi \phi^*(a,b) = \int_0^{2\pi} \phi^*(t) |a|^{-\frac{1}{2}} \left[1-\left(\frac{t-b}{a}\right)^2\right] e^{-\frac{\left(\frac{t-b}{a}\right)^2}{2}} dt \tag{5}$$

With $\phi^*(t) = \phi(l) + t$ and $t = \frac{2\pi l}{L}$ we receive consequently Equation (6).

$$W_\Psi \phi^*(a,b) = a^{\frac{-1}{2}} \int_0^L \left[\phi(l) + \frac{2\pi l}{L}\right] \cdot \left[1-\left(\frac{\frac{2\pi l}{L}-b}{a}\right)^2\right] e^{-\frac{\left(\frac{\frac{2\pi l}{L}-b}{a}\right)^2}{2}} \frac{2\pi}{L} dl \tag{6}$$

This Equation can be modified after multiplication of the terms to the following Equation

$$W\Psi\phi^*(a,b)=\frac{2\pi}{L}a^{\frac{-1}{2}}\left[\int_0^L \phi(l)e^{-\frac{1}{2}\left(\frac{2\pi l-bL}{aL}\right)^2}dl + \int_0^L \frac{2\pi l}{L}e^{-\frac{1}{2}\left(\frac{2\pi l-bL}{aL}\right)^2}dl - \int_0^L \phi(l)\left(\frac{2\pi l-bL}{aL}\right)^2 e^{-\frac{1}{2}\left(\frac{2\pi l-bL}{aL}\right)^2}dl - \int_0^L \frac{2\pi l}{L}\left(\frac{2\pi l-bL}{aL}\right)^2 e^{-\frac{1}{2}\left(\frac{2\pi l-bL}{aL}\right)^2}dl\right] \quad (7)$$

Equation (7) includes four terms, which we denote with T1-T4. One note that T2 and T4 are independent on the function $\phi(l)$ and their computation yield to constant values (see Equation (8) and (9)).

$$T2=\frac{aLb}{2\sqrt{2\pi}}erf(z_n)-\frac{aLb}{2\sqrt{2\pi}}erf(z_0) - \frac{a^2L}{2\pi}e^{-z_n{}^2}+\frac{a^2L}{2\pi}e^{-z_0{}^2} \quad (8)$$

$$T4=\frac{a^2L}{\pi}\left(z_n^2+\frac{b}{a\sqrt{2}}z_n+1\right)e^{-z_n^2} - \frac{a^2L}{\pi}\left(z_0^2-\frac{b}{a\sqrt{2}}z_0+1\right)e^{-z_0^2} - \frac{abL}{2\sqrt{2\pi}}erf(z_n)+\frac{abL}{2\sqrt{2\pi}}erf(z_0) \quad (9)$$

with $z_0=\frac{1}{\sqrt{2}}\left(\frac{-b}{a}\right)$ and $z_n=\frac{1}{\sqrt{2}}\left(\frac{2\pi-b}{a}\right)$

The other two terms T1 and T3 depend on the transformation function and can't be calculated directly. Since the function $\phi(l)$ is constant along the polygon edges, the terms T1 and T3 can be calculated through dividing the interval $[0-2\pi]$ into several intervals according to the number of polygon edges. The first term T1 can be written as following:

$$T1=\int_0^{l_1}\phi(l_1)\,e^{-\frac{1}{2}\left(\frac{2\pi l-bL}{aL}\right)^2}dl \quad \ldots \quad + \int_{l_{n-1}}^{l_n=L}\phi(l_n)\,e^{-\frac{1}{2}\left(\frac{2\pi l-bL}{aL}\right)^2}dl \quad (10)$$

Where l_i and $\phi(l_i)$ are the length of the polygon edge i and the angle differences between the edges i and i+1. In the interval $[l_{i-1}-l_i]$ the angle difference is consequently constant. Equation (10) can be therefore modified to:

$$T1=\phi(l_1)\int_0^{l_1}e^{-\frac{1}{2}\left(\frac{2\pi l-bL}{aL}\right)^2}dl \quad \ldots \quad +\phi(l_n)\int_{l_{n-1}}^{l_n=L}e^{-\frac{1}{2}\left(\frac{2\pi l-bL}{aL}\right)^2}dl \quad (11)$$

Using the parameter transformation

$$z_i=\frac{1}{\sqrt{2}}\left(\frac{2\pi l_i-bL}{aL}\right)$$

Equation (11) can be written as given below.

$$T1=\frac{aL}{\sqrt{2\pi}}\left[\phi(l_1)\int_{z_0}^{z_1}e^{-z^2}dz\ldots+\phi(l_n)\int_{z_{n-1}}^{z_n}e^{-z^2}dz\right] \quad (12)$$

With $\int e^{-z^2}dz=\frac{1}{2}\sqrt{\pi}\,erf(z)$

we receive finally

$$T1=\frac{aL}{2\sqrt{2\pi}}\left[\phi(l_1)\left(erf(z_1)-erf(z_0)\right)+\ldots + \phi(l_n)\left(erf(z_n)-erf(z_{n-1})\right)\right] \quad (13)$$

Through multiplication and rearranging we get the final expression for the first term of Equation (7).

$$T1=\left[\frac{aL}{2\sqrt{2\pi}}\left(erf(z_n)-erf(z_0)\right)\phi(l_1) - \frac{aL}{2\sqrt{2\pi}}\sum_{i=1}^{n}erf(z_i)\alpha_i - aL\sqrt{\frac{\pi}{2}}\,erf(z_n)\right] \quad (14)$$

Where α_i is the angle difference between the polygon edges *i* and *i+1*.

In similar way we obtain for the third term T3 the following expression:

$$T3=T1-\frac{aL}{\sqrt{2\pi}}\left(z_0e^{-z_0{}^2}-z_ne^{-z_n{}^2}\right)\phi(l_1) - \frac{aL}{\sqrt{2\pi}}\sum_{i=1}^{n}z_ie^{-z_i{}^2}\alpha_i - \sqrt{2}aLz_ne^{-z_n{}^2}\Big] \quad (15)$$

Using Equation (8) (9) (14) and (15) the CWT delivers finally the wavelet coefficients as given in Equation (16).

$$W_\Psi f(a,b) = -\frac{aL}{\sqrt{2\pi}}\left(z_0 e^{-z_0^2} - z_n e^{-z_n^2}\right)\phi(l_1)$$
$$-\frac{aL}{\sqrt{2\pi}}\sum_{i=1}^{n} z_i e^{-z_i^2}\alpha_i$$
$$-\frac{aL}{\sqrt{2\pi}}\sum_{i=1}^{n} z_i e^{-z_i^2}\alpha_i$$
$$+\frac{aLb}{\sqrt{2\pi}}erf(z_n)$$
$$-\frac{aLb}{\sqrt{2\pi}}erf(z_0)$$
$$+\left(-\frac{a^2L}{\pi}z_n^2+\frac{aL(2\pi-b)}{\sqrt{2\pi}}z_n-\frac{3a^2L}{2\pi}\right)e^{-z_n^2}$$
$$+\left(\frac{a^2L}{\pi}z_0^2-\frac{aLb}{\sqrt{2\pi}}z_0+\frac{3a^2L}{2\pi}\right)e^{-z_0^2} \qquad (16)$$

4. WAVELET DESCRIPTORS

To apply wavelet descriptors to represent a given object we vary the values of the compression or dilatation parameter *a* and the shifting parameter *b* in Equation (4) to receive a sufficient set of Mexican Hat functions within the interval $[0-2\pi]$. Fig. 5 shows a part of the wavelet building set used in our application.

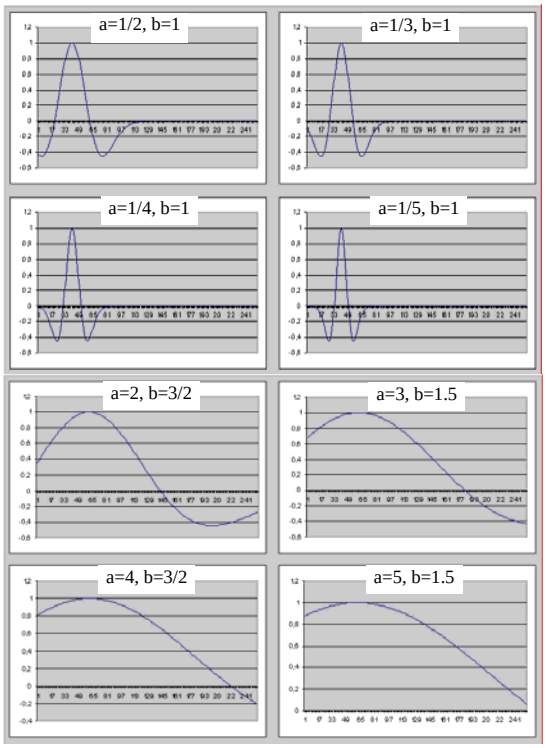

Fig. 5 Part of the wavelet building set applied for the Mexican Hat function in the interval $[0-2\pi]$

As shown in this Figure the small values of the parameter *a* ($a < 1$) produce compressed variants of the Mexican Hat function and are qualified to describe the details of the contour shape. Big values on the other hand create dilated variants of the same function and are used to approximate the object shape. It is clear that the higher the number of the descriptors is, the more particular the representation of the object shape is. Fig. 6 shows for example an image with different classes of weed species. The corresponding 16 Fourier (FD) and wavelet descriptors (WD) for the first two weed of the class VER are given in Fig. 7.

VER THL POA STE CAP LAM MAT GAL

Fig. 6 Example of different classes of weed species

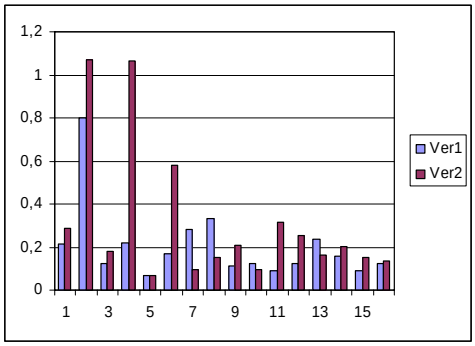

(a)

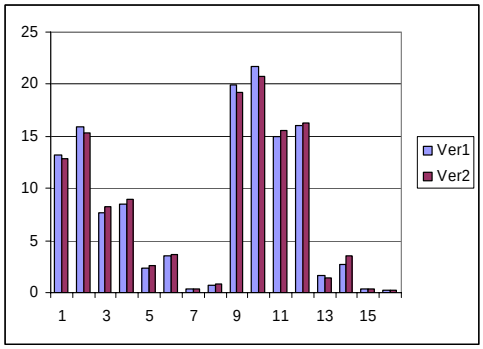

(b)

Fig. 7 a) Fourier descriptors (FD), b) wavelet descriptors (WD) of the weed species VER

The first half of the WD shown in Fig. 7b [WD_1-WD_8] represents the wavelet coefficients which are calculated for the parameters $a \in \{2,3\}$, $b \in \{-2,-1,0.5,1\}$ and used as approximation signal ($a > 1$). The second half [WD_9-WD_{16}] represents the wavelet coefficients which are calculated for the parameters $a \in \{0.5,0.125\}$, $b \in \{-2,-1,0.5,1\}$ and corresponds to a detail signal ($a < 1$). It is important to mention here that the values of the FD in comparison with the values of the WD are invariant with respect to the starting point on the contour.

To calculate the differences between two object shapes we use the minimum distance (d) as given in the following Equation:

$$d = \sqrt{\sum_{1}^{n} \left(WD_i - WD_i' \right)^2} \qquad (17)$$

It is easy to see that the differences between the FD are greater than the differences of the WD for the given example (see Fig 7). Specially for the low frequent FD and WD. This can cause confusion between objects in recognition tasks when we use the WD instead of the FD. To study the behaviour of the WD for more coefficients we calculated 256 FD and WD for the same weed species of Fig. 6. Fig. 8 shows these results.

As shown in Figure 8a the values of the FD decrease for high frequencies rapidly, so that the differences between the FD of different objects also decrease. The values of the WD indicate a periodical behaviour. Therefore it is not necessary for recognition tasks to use all WD to represent a given object, since only a few number of WD are needed and qualified to recognize the object.

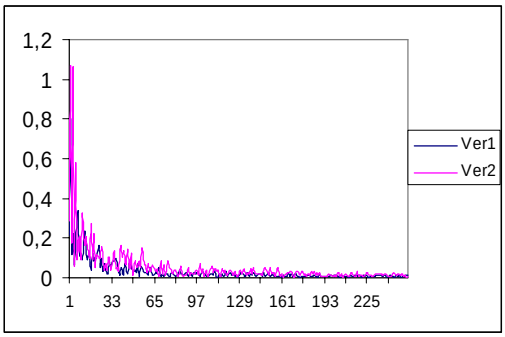

(a)

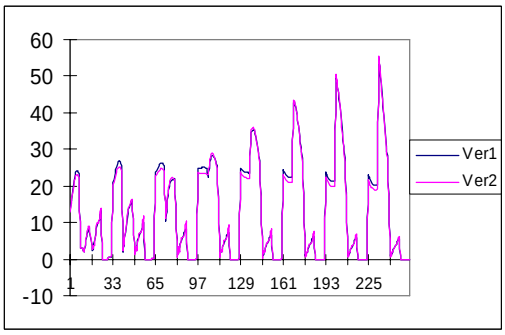

(b)

Fig. 8 256 FD (a) and WD (b) of the objects in Figure 5

5. CONCLUSION

The representation of object contours using wavelet descriptors is useful in view of object recognition tasks. In particular, the Mexican Hat function is qualified to be used as mother wavelet to apply a number of WD using only the polygon parameters. The number of WD needed to recognize given objects increases according to the complexity of the object shapes. Certainly it is necessary to study the influence of choosing the starting point on the recognition process, since the values of the WD depends on it. This task will be investigated in features works.

REFERENCES

Freeman H. (1974). Computer processing of line-drawing images, pp. 57-97, Computer Surveys, **6**.

Ramer U. (1972). An iterative procedure for the polygonal approximation of plane curves, pp. 244-256, Comp. Graphics and Image Proc., **1**.

Rodenacker, K., P. Bischo and B.B. Chaudhuri (1987). Featuring of topological characteristics in digital images, pp. 945–950, Acta Stereol, **6**, no. Suppl III.

Granlund G. H., (1972). Fourier preprocessing for hand print character recognition, pp. 195-201, IEEE Trans. On C-**21**.

Chunag G.C.-H., C.-C. Jay Kuo, (1996). Wavelet Descriptor of Planar Curves: Theory and Applications, *IEEE Transaction on Image Processing*, **5**.

Feng L., T. D. Bui, (2001). Classification of Similar 2-D Objects by Wavelet-Sparse-Matrix (WSM) Method, pp. 329-345, *International Journal of Pattern Recognition and Artificial Intelligence*, **15**, No. **2**.

Zahn C., R.Z Roskies, (1972). Fourier descriptors for plant closed curve, IEEE Trans. On C-**21**.

Nabout A., (1992). Modulares Konzept und Methodik zur wissensbasierten Erkennung komplexer Objekte in CAQ-Anwendungen, Diss., Universität Wuppertal, Fachbereich Elektrotechnik, Germany.

Nabout A., H.A. Nour Eldin, R. Gerhards, B. Su, W. Kühbauch, (1994). Plant Species Identification using Fuzzy Set Theory, pp. 48-53, Proc. of the IEEE Southwest Symposium on Image Analysis and Interpretation, Dallas, Texas, USA.

Nabout A., B. Su, H.A Nour Eldin, (1995). A Novel Closed Contour Extractor, Principle and Algorithm, pp.445-448, Proc. of the IEEE International Symposium on Circuits and Systems ISCAS '95, Seattle, WA, USA.

Nabout A., H.A. Nour Eldin, (1993). The topological contour closure requirement for object extraction from 2D-digital images, pp120-125, IEEE International Conference on Systems, Man and Cybernetics, vol. **3**, Le Touquet, France.

Nabout A., B. Su, H.A. Nour Eldin, (1995). Measurement of Ring-Shaped and Toothed Mechanical Parts through Image Processing, pp. 396-401, Proc. of the IEEE Instrumentation and Measurement Technology Conference IMTC/95, Waltham, MA, USA.

Strang, G., (1993) Wavelet transforms Fourier transforms, *Bullettin (New Series) of the American Mathematical Society*, **28**.

Daubechies, I., (1992). Ten Lectures on Wavelets, *Society for Industrial & Applied Mathematics*.